Available online at www.sciencedirect.com

ScienceDirect

journal homepage: www.elsevier.com/locate/he

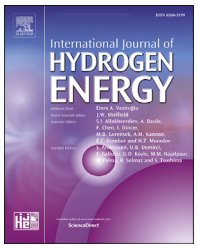

Hydrogen permeation studies of composite supported alumina-carbon molecular sieves membranes: Separation of diluted hydrogen from mixtures with methane

Margot A. Llosa Tanco [a,**], *Jose A. Medrano* [b], *Valentina Cechetto* [b], *Fausto Gallucci* [b,*], *David A. Pacheco Tanaka* [a]

[a] *TECNALIA, Basque Research and Technology Alliance (BRTA), Mikeletegi Pasealekua 2, 20009, Donostia, San Sebastián, Spain*

[b] *Inorganic Membranes and Membrane Reactors, Department of Chemical Engineering and Chemistry, Eindhoven University of Technology, Eindhoven, the Netherlands*

HIGHLIGHTS

- Al-CMSM membranes carbonized at 500 °C were successfully prepared.
- Perm-selectivity/permeability properties of the membrane are placed above the Robeson limit.
- The membrane was successfully tested for the separation of low concentration of H_2.
- H_2 purity was 99.4% making this membrane a good candidate for the separation of H_2.

ARTICLE INFO

Article history:
Received 6 February 2020
Received in revised form
12 April 2020
Accepted 9 May 2020
Available online 24 June 2020

Keywords:
Hydrogen separation
Carbon membrane
Hydrogen-methane mixture
Low concentration hydrogen

ABSTRACT

One alternative for the storage and transport of hydrogen is blending a low amount of hydrogen (up to 15 or 20%) into existing natural gas grids. When demanded, hydrogen can be then separated, close to the end users using membranes. In this work, composite alumina carbon molecular sieves membranes (Al-CMSM) supported on tubular porous alumina have been prepared and characterized. Single gas permeation studies showed that the H_2/CH_4 separation properties at 30 °C are well above the Robeson limit of polymeric membranes. H_2 permeation studies of the H_2–CH_4 mixture gases, containing 5–20% of H_2 show that the H_2 purity depends on the H_2 content in the feed and the operating temperature. In the best scenario investigated in this work, for samples containing 10% of H_2 with an inlet pressure of 7.5 bar and permeated pressure of 0.01 bar at 30 °C, the H_2 purity obtained was 99.4%.

* *Corresponding author.*
** *Corresponding author.*
E-mail addresses: margot.llosa@tecnalia.com (M.A. Llosa Tanco), f.gallucci@tue.nl (F. Gallucci).

https://doi.org/10.1016/j.ijhydene.2020.05.088

Introduction

The so-called hydrogen economy is based on the clean conversion of hydrogen to electricity, releasing water as the only by-product. The energy density of H_2 is higher than traditional fuels and it can be fed to fuel cells to produce electrical energy. H_2 can also be used as energy carrier for renewable sources by converting surplus power to H_2 via electrolysis. The centralized production of H_2 requires storage, distribution and transportation infrastructures to deliver it to the end users, which result in a significant cost increase as these infrastructures are not existing. This cost can be greatly reduced by blending H_2 into the existing natural gas storage and distribution infrastructures [11]. The safety risk increased by blending H_2 into natural gas pipeline systems is related to the H_2 content in the gas mixtures, and this risk increase is acceptable for H_2 addition up to 15–20%. In this way, pure H_2 can be delivered to the multiple customers by using separation technologies close to the end users. H_2 separation by selective membranes is a promising technology for the recovery of H_2 present in low concentrations in the feed. For this application, membranes with high permeation flux and high selectivity, above the upper bound Robeson's limit for polymeric membranes are required. Among all membranes proposed for this separation, Pd based membranes and Carbon Molecular Sieves Membranes (CMSMs) are good alternatives.

Pd and Pd alloy membranes have high H_2 permeation and very high selectivity due to their unique chemical-adsorption/diffusion mechanism: H_2 is adsorbed on the surface, then dissociated into hydrogen atoms, and finally they permeate through the membrane bulk. The permeation follows the Sieverts law, which depends on the temperature, thickness of the membrane and the difference in the square root of the pressures in both sides of the membrane. In order to reduce the costs (Pd is expensive), increase the permeation and reduce the number of membranes; thin membranes (<5 μm) are being developed [4,5,10,13]. In these membranes, the competition of any compound with H_2 for the active sites on the surface of the membrane can alter significantly the permeation flux. The effect of competitive adsorption depends on various factors such as inhibitor affinity, temperature and H_2 partial pressure. Also H_2S interacts strongly with Pd, thus reducing considerably the permeation. Depending on the H_2S concentration and temperature, the reaction can be irreversible through the formation of the PdS_4, which is not permeable to H_2 and can even destroy the membrane [12]. For ultra-thin Pd membranes, CO interaction is significant and even CO_2 can reduce the permeation [13]. Apart from the competition between species for permeation, the main drawback of pure Pd membranes is that they are damaged by H_2 embrittlement due to the α-β phase transition of Pd hydride at below the critical temperature (300 °C) and pressure (2 Mpa). This implies that H_2 need to be separated at temperatures well above the ambient with the need of heating elements. Still, if permeation is to be considered at around 300 °C, at those temperatures the permeation decreases considerably [15]. Additionally, as the permeation depends on the square root of the pressure, at high pressures the increment in the permeation with the pressure is not high.

Carbon molecular sieve membranes (CMSM) are produced by the carbonization of polymeric precursors under an inert atmosphere or vacuum. These membranes have microporous structures which can discriminate gases by molecular sieving based on the size and shape of the molecules by ultramicropores (<0.7 nm) and selective surface diffusion through larger micropores (~0.7–2 nm) where the more adsorbable gas on the high-pressure side of the membrane selectively adsorbs onto the surface and diffuses across the surface of the pores to the low pressure side; by this mechanism, the membranes can separate non-adsorbable or weakly adsorbable gases from adsorbable gases. Furthermore, CMSM can operate at low temperatures, hence they can be rapidly implemented in the natural gas grid.

In order to increase the permeation and selectivity of the CMSM, composite inorganic-CMSM were developed. Some of us reported for the first time the preparation of a 7 cm long, 1 cm diameter-supported composite alumina-CMSM (Al-CMSM) from low cost polymer precursors phenolic resins: resol [18–20] and novolac [8,9] in one dip-dry-carbonization cycle. The membranes obtained from both precursors were found to have a thickness of around 3 μm and with their pores hydrophilic, which can adsorb water molecules reducing thus the pore size; this physisorbed water can be removed by heating [9].

The effect of the carbonization temperature on the pore size and pore size distribution of the Al-CMSM obtained from novolac resin showed that the proportion of ultramicropores, responsible of molecular sieving mechanism, increases with the temperature of carbonization. On the other hand, the proportion of the intermediate size micropores (0.5–0.8 nm), responsible of adsorption diffusion mechanism, decreases at carbonization temperatures higher than 650 °C. The membranes carbonized at less than 550 °C show H_2/N_2 permeation properties that are above the Robeson upper bound plot [9]. Unlike Pd, phenolic resins are cheap, the gas permeation is proportional to the difference of pressure difference across the membrane and they are less susceptible to surface contamination.

Recently Kumakiri et al. [7] studied the influence of the addition of iron to CMSM prepared from a lignin-based material and phenolic resin as precursors. The authors found that adding iron (III) acetate to the precursors, H_2 selectivity increased significantly (H_2/CH_4 from 54 to 584) while maintaining H_2 permeability (1.69 and 1.32×10^{-7} mol m^{-2} s^{-1} Pa^{-1}, respectively). Ngamou et al. [14] reported the preparation of an ultrathin (~200 nm) CMSM, from a polyimide precursor carbonized at 700 °C, on the inner surface of an α-Al_2O_3/γ-Al_2O_3 tubular support, the membrane showed very high single H_2 permeance (1×10^{-6} mol m^{-2} s^{-1} Pa^{-1}) and perm-selectivity for H_2/CH_4 (228) at 200 °C, showing the potential of these membranes for high temperature H_2 purification.

In general, membrane permeation characteristics (permeability and perm-selectivity) are based on single gas permeation tests for different gases. However, limited information is available in the literature on the gas separation of gas mixtures and the mutual interaction of the gases through the pores.

In this work, a supported composite Al-CMSM obtained from novolac resin prepared by the one dip-dry-carbonization

step carbonized at 500 °C was prepared and the He, H_2, CO_2, N_2 and CH_4 single gas permeation properties evaluated. Then, H_2 separation from a mixture with CH_4 containing less than 20% of H_2 has been studied, and the effect of the hydrogen content, temperature, and pressure on hydrogen purity has been assessed.

Materials and methods

Membrane preparation and characterization

Al-CMSM were prepared using the materials and the one dip-dry-carbonization method on porous alumina supports described elsewhere [8,9].

Preparation of the support

Both ends of a porous tubular asymmetric alumina support from Inopor (200 nm pore size in the outer surface, 10 mm o. d. And 7 mm i. d.) were connected to non-porous alumina tubes with a glass sealant at 1150 °C, one end was open and the other was close; the surface of both ends was covered with glass leaving an effective length of 150 mm (See Fig. 1).

Preparation of the dipping solution

Novolac phenol-formaldehyde resin synthesized by the acid-catalyzed phenol-formaldehyde condensation and Boehmite (10 wt%) particle size 8–18 nm (supplied by Kawaken Fine Chemicals) were used as the sources of carbon and alumina respectively. The solution containing resin (13 wt%), formaldehyde (2.4 wt%), ethylenediamine (0.6 wt%), boehmite solution (0.8 wt%) and 83 g of *N*-methyl-2-pyrrolidone (NMP) was heated for 2 h at 100 °C before dipping.

Preparation of the membrane

The support was immersed for 10 s in the dipping solution, dried at 100 °C overnight under continuous rotation inside an oven. Then, the membrane was carbonized under N_2 at 500 °C for 2 h, the heating rate was 1 °C min^{-1}.

SEM characterization

The thickness of the membrane was determined using a FEI Quanta 250 FEG (ESEM).

Permeation experiments

The permeation measurements just after carbonization were carried out at room temperature using a shell-and-tube reactor [16]. For the other permeation experiments, the dense alumina tubes of both ends were removed and sealed with standard Swagelok connections and graphite ferrules [3]. One side of the membrane was connected to a 6-mm stainless steel (SS) tube and the other side was closed leading to a dead-end configuration. Since these membranes are meant for low temperature applications, gas-tight resin has also been applied in the connections to make sure that gas leaks are avoided. The membrane was placed into a 4.5 cm inner diameter stainless steel tube reactor; the reactor assembly was set inside an electrical oven to control the permeation temperature. The flux of the gases is controlled by flow controllers (Bronkhorst). Since the permeation of the carbon membranes depends on the water adsorbed in the pores, the

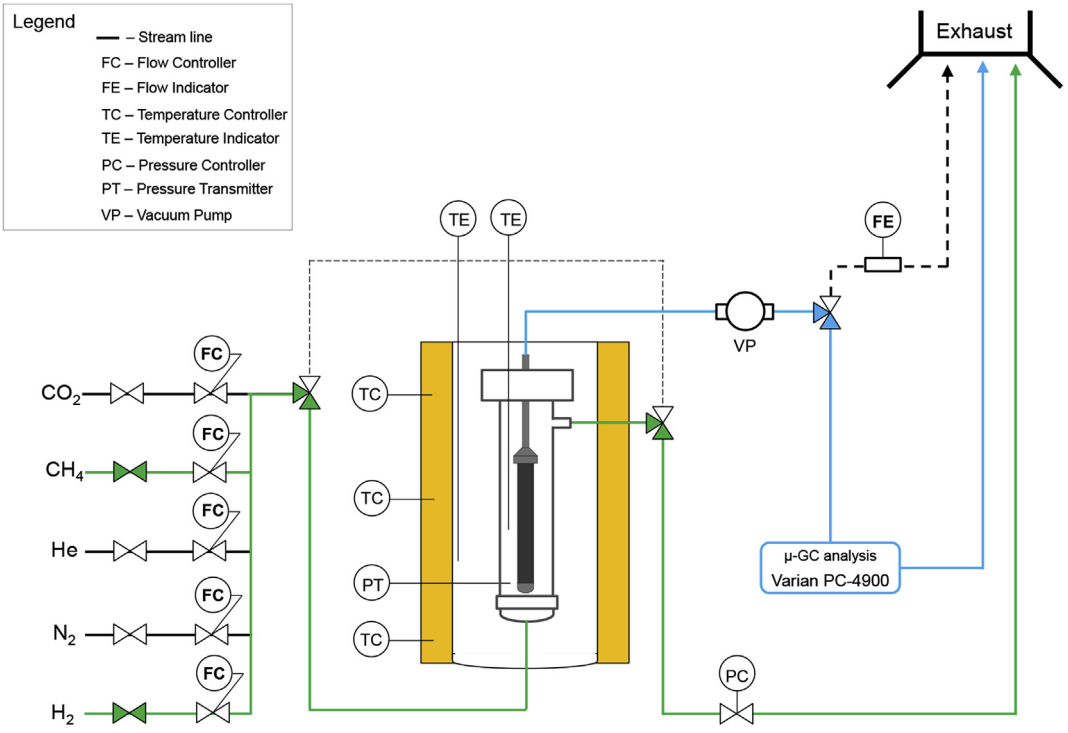

Fig. 1 – Schematic representation of the permeation set-up.

membrane was activated by heating at 100 °C and 4 bar in He following the procedure suggested elsewhere [8].

The experimental setup used in this work, together with all the instrumentation installed through the setup is schematically represented in Fig. 1. Downstream the permeation vessel there is a back-pressure regulator that controls the feed pressure. On the other hand, the permeate is connected to a diaphragm vacuum pump (model VWR PM20404–820.3) to maximize the partial pressure between feed and permeate; the vacuum in the permeated was 0.01 atm. From the outlet of the vacuum pump, already at atmospheric pressure, the gas is sent either to a film-flow meter (Horiba Stec VP3) or to a micro-GC (model Varian CP-4900) to measure the gas composition. In this case the selectivity to H_2 separation $S_{H2/CH4}$ is measured as presented in Eq. (1).

$$S_{H_2/CH_4} = \left(\frac{\%H_{2,perm}}{\%CH_{4,perm}}\right) \cdot \left(\frac{\%CH_{4,feed}}{\%H_{2,feed}}\right) \quad (1)$$

Single gas permeation experiments were carried out first for different gases with different kinetic diameters. Subsequently, the permeation of different H_2/CH_4 mixtures at different operating conditions has been investigated. An overview of the different experiments performed in this work is depicted in Table 1.

Results and discussion

Llosa Tanco and coworkers reported previously in the literature the preparation and characterization of 50 mm long Al-CMSM using the same materials and method [8,9]. However, in this work five membranes of 150 mm long (three times longer) were prepared. Single gas permeation test showed that the five membranes prepared have similar properties in terms of permeance, indicating the reproducibility of the method. Therefore, in this work, all the experiments were carried out using one membrane. The thickness of the membrane determined by SEM is 3 μm (Fig. 2), equal to those (50 mm long) reported before.

Just after removing the membrane from the carbonization oven (preventing the contact with water from the air), the N_2 permeation at room temperature was measured, showing a permeance of 1.62×10^{-7} mol m^{-2} s^{-1} Pa^{-1}. After leaving the membrane for several weeks exposed to ambient conditions, the N_2 permeance decreased to 3.8×10^{-10} mol m^{-2} s^{-1} Pa^{-1}. During the carbonization, the polymer decomposed leaving pores with reactive carbons atoms which react with water from the air producing hydrophilic groups on the pores; then, physisorption of water in the pores occurred, leading to a decrease in the pore size [9]. The pores of the Al-CMSM were partially open by heating the membrane under He, at 4 bar pressure difference (He was used because it does not adsorb on the pores and the permeation is higher than N_2); the He flow increases with the temperature from 98 mL min^{-1} at 32 °C to 137 mL min^{-1} at 100 °C (Figure S1) due to the removal of some water adsorbed in the pores. The activation was carried out to increase the permeation of gases.

Table 1 – Overview of the experimental conditions investigated in this work.

Overview of the experiments	
Experimental conditions	
Activation temperature [°C]	100
Permeation temperature [°C]	30–40 – 60–80
Pressure feed [bar]	4–7.5
Pressure permeate [bar]	0.01
Single gases measured and compositions of the gas mixtures	
Single gases investigated	He, H_2, CO_2, N_2, CH_4
H_2/CH_4 compositions [%]	5/95; 10/90; 20/80

Single gas permeation studies

After the activation, the temperature was decreased to 30 °C (under He), then single gas permeation of He, N_2, H_2, CO_2, and CH_4 at various pressures and temperature were carried out; the pressure inside the tube was atmospheric pressure. From the flow rates, membrane surface area and pressure, the permeance values were calculated. For a given temperature and gas, the average permeance was considered and the results are listed in Table 2.

Fig. 3 shows the permeance at various temperatures of He, H_2, CO_2, N_2 and CH_4 as a function of the kinetic diameter. The permeance pattern is similar to those reported before [9] using the same method of fabrication but for membranes carbonized at 500 °C, showing the reproducibility of the method of preparation of the membranes. From CH_4 to H_2, as the kinetic diameter decreases, the permeance of the gas increases; this is an indication of the contribution of the molecular sieving separation by the Al-CMSM. However, the permeance of H_2 is higher than the smaller He; this behavior is attributed to a) the smaller cross-section diameter of H_2 and b) the higher

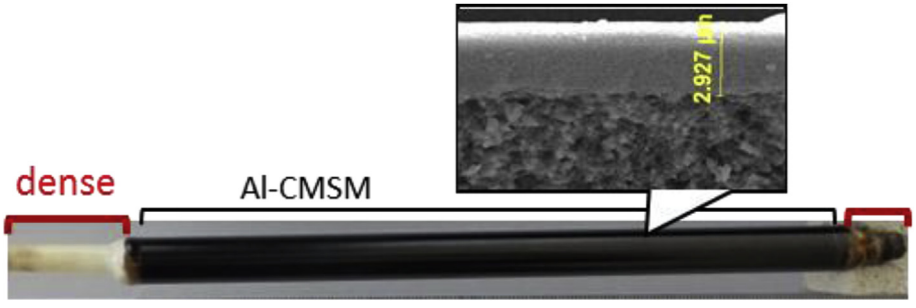

Fig. 2 – Al-CMSM on porous alumina support.

Table 2 – Kinetic diameter, permeance of various gases at different temperatures and activation energy calculated from slope of the Arrhenius plot.

	He	H_2	CO_2	N_2	CH_4
Kinetic diameter [nm]					
	0.26	0.29	0.33	0.365	0.38
Temperature [°C]			Permeance x 10^{-9} [mol s^{-1} m^{-2} Pa^{-1}]		
30	50.4	108.7	10.9	1.72	0.25
40	52.4	118.5	14.9	2.36	0.28
60	56.9	127.6	28.7	3.58	0.82
80	62.6	149.3	49.9	8.74	4.08
Activation energy [kJ mol^{-1}]					
	3.8	5.3	27.3	27.7	61.6[a]

[a] Calculated using permeances at 40, 60 and 80 °C.

interaction (adsorption) of H_2 with the hydrophilic pores which enhances the adsorption-diffusion transport mechanism.

From the permeance data at different temperatures, using the slope of the Arrhenius plot (Fig. 4), the apparent activation energy (Ea) for the permeation of the gases was calculated and the results are listed in Table 2. For CH_4, the permeances at 30 and 40 °C are similar (Table 1); the big difference is observed between of 40 and 80 °C where the CH_4 in the gas phase is much higher than the adsorbed (below, this statement will be explained in more detail), therefore, these three temperatures were used for the calculation of Ea, of CH_4.

The activation energy values may help to determine the size of the necks (responsible of molecular sieving) in the CMSM. As the pore size decreases, it is more difficult for the gas to pass through, requiring more energy for permeation. In Fig. 5, the Ea of permeation as function of the kinetic diameter of the gases is shown; it is observed that Ea increases with the diameter of the gases. For He and H_2 the Ea is small, which indicates that the pores are much bigger than the kinetic diameter of the gases; therefore, they can pass through the membrane easily. From N_2 to CH_4, there is a sharp increase of Ea, suggesting that most of the necks are around 0.36 nm, the size of N_2. The Ea of CO_2 is higher than expected considering only the gas kinetic diameter size. CO_2 is also adsorbed in the large hydrophilic micropores consequently, the activation energy observed is the result of the addition of molecular sieving and adsorption diffusion mechanisms. For similar membranes carbonized at 500 °C, it was reported that between 160 and 180 °C, the adsorption-diffusion mechanism for CO_2 is not relevant and the predominant mechanism is molecular sieving [8]. Similarly, the high value of Ea measured for CH_4 can also be attributed to the combined effect of molecular sieving and the adsorption of CH_4 in the large pores, which normally occurs at temperatures of around 60 °C. This would explain the sharp increase observed in both CO_2 and CH_4 (Fig. 6b) compared to the expected trend followed by He, H_2 and N_2.

H_2 and CH_4 single gas permeation flow rates at various pressures and temperatures are shown in Fig. 6 (pressure in the permeate side is kept at atmospheric conditions). For hydrogen, as it is expected, the flow increases with the pressure and temperature. On the other hand, the flow of CH_4 at 40 °C is slightly higher than at 30 °C, the flux increases at 60 °C and the difference is much higher between 60 and 80 °C (Table 1). Ma et al. [1,17] studied the permeability properties of He, H_2, CO_2, O_2 and CH_4 microporous silica membranes as a function of pressure and temperature; the authors reported that for each diffusing gas a temperature exists at which the amount of the adsorbed phase inside the pores equals to the gas

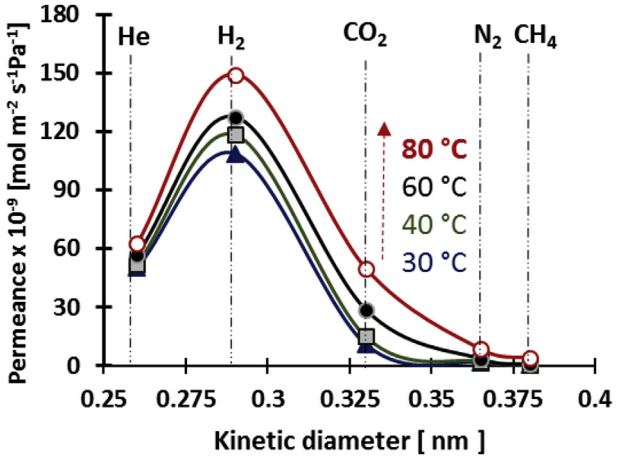

Fig. 3 – Permeance of various gases in function of their kinetic diameter at various temperatures.

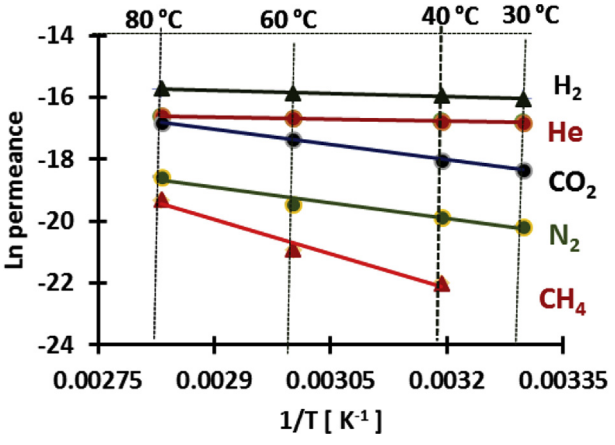

Fig. 4 – Arrhenius plot for various gases.

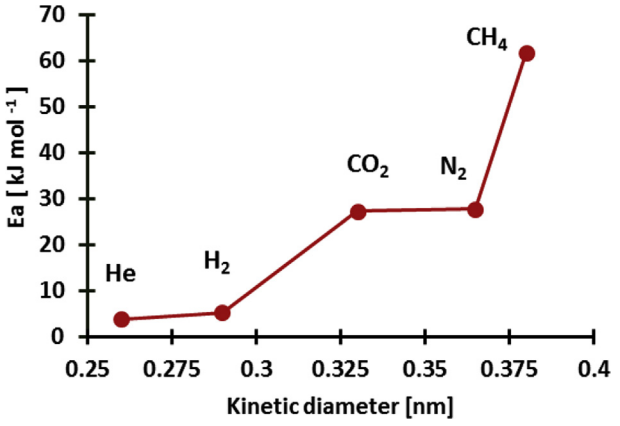

Fig. 5 – Activation energy (Ea) in function of the kinetic diameter of the gases.

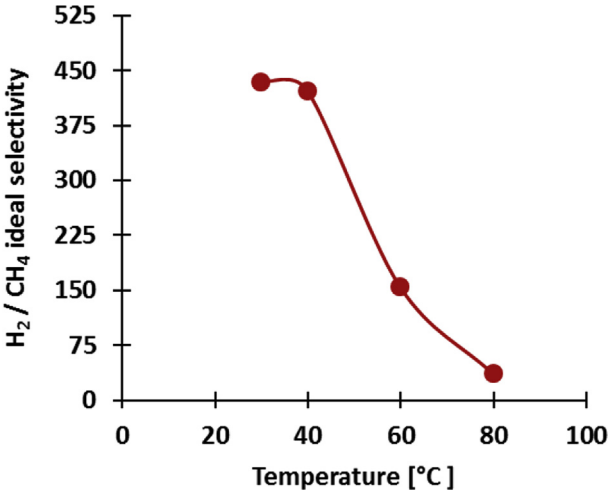

Fig. 7 – H_2/CH_4 ideal selectivity calculated from single gas permeances at various temperatures.

amount in the non-adsorbed gas phase (iso-concentration point, ICP). If the temperature is increased 20 °C above this point, the amount of adsorbed gas decrease by 1 order of magnitude in comparison to the concentration in the gas phase. For their membranes, the ICP temperatures for CH_4 and CO_2 were 70 and 160 °C respectively; permeation studies on Al-CMSM for CH_4 and for CO_2 reported before by some of us [8] suggest that the ICP values are quite similar. Between 60 and 80 °C, the CH_4 adsorbed is very small compared to that in the gas phase, therefore, at these conditions, the permeation mechanism is mainly molecular sieving, while at lower temperatures the combined molecular sieving and adsorption-diffusion mechanism occurs, which in its turn leads to a sharp decrease in the CH_4 permeation through the membrane at temperatures below 80 °C.

From H_2 and CH_4 single gas permeance at various temperatures (Table 2), the ideal H_2/CH_4 perm-selectivities were calculated and the values are displayed in Fig. 7. It can be observed that the ideal selectivity decreases with the temperature; from 435 at 30 °C to 37 at 80 °C, owing mainly to the sharp increase of the CH_4 permeation.

In the last years, other carbon membranes have been prepared and investigated in the literature for single gases, although never in the case of gas mixtures. For instance Ref. [2], investigated the use of cellophane as precursor for the carbon membranes, and they found micropores in the range of 0.3–0.8 nm. Hosseini et al. [6], also investigated the influence of the carbonization temperature of poly (benzimidozale) PBI and polyimides precursors, finding that the ideal perm-selectivity surpassed the trade-off lines of several industrial gas mixtures. Recently [21], investigated the addition of a thin TiO_2 layer in between the alumina support and the carbon layer in order to increase the adhesion strength of the carbon membrane with the support material. These authors compared the performance of their membranes with other membranes previously reported in the literature.

In order to compare the performance of the membrane tested in this work using novolac as precursor material, an updated Robeson plot including the trade-off of the polymeric membranes and another one of carbon membranes is represented in Fig. 8. From this figure, it is evidenced that the

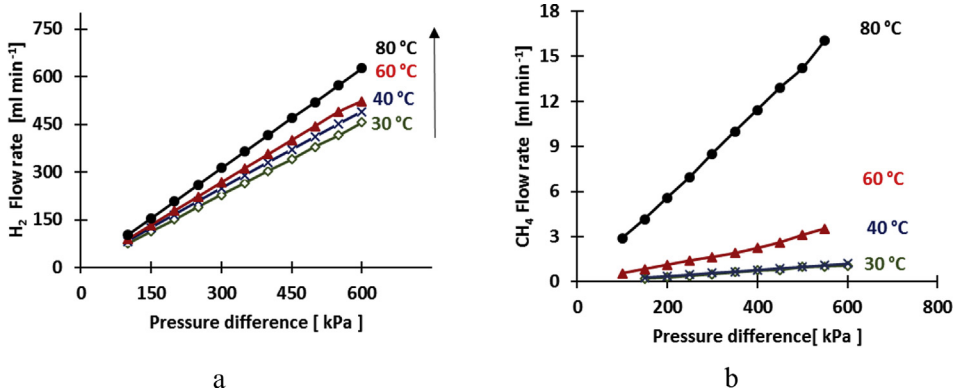

Fig. 6 – a) hydrogen and b) methane flow rates at various pressures and temperatures. (the flow rate at 30 and 40 °C are very close to each other).

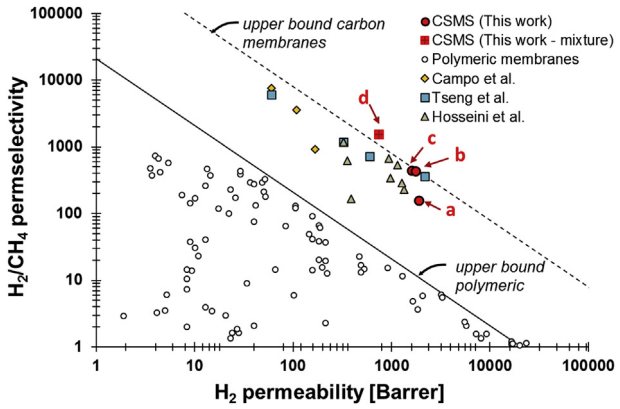

Fig. 8 – Revised Robeson upper bound plot including the upper bound of carbon membranes for H_2/CH_4 for the Al-CMSM at different temperatures and comparison with some of the results found with polymeric membranes located in the upper bound. a, b and c this work from single gas permeation at 60, 40 and 30 °C respectively. d, this work from Table 4 at 30 °C.

results of this work lay on the upper bound and that in case of using gas mixtures, the results can overcome this barrier.

Hydrogen separation from a mixture with CH_4 containing less than 20% of H_2

In order to set these results in context, the main objective of the Hygrid project (funded by the EU Fuel Cells and Hydrogen 2 Joint Undertaking and the EU Horizon 2020) is to use the existing infrastructure of natural gas grid to storage and distribute hydrogen present at low concentrations (<20%); then, the hydrogen is separated at the end users using a membrane based technology. Hydrogen separation from inlet mixtures of CH_4 containing 5, 10 and 20% of H_2 at 7.5 bar pressure and 2000 ml min^{-1} flow rate at 80 and 40 °C and applying vacuum in the permeate (0.01 bar) were carried out and the results are listed in Table 3 the observed values are experimental, while the calculated ones were predicted from single gas permeances data given in Table 2. It can be observed that the permeate flow increases with the H_2 concentration and the temperature since H_2 has higher permeance than CH_4 and the permeation of both gases increases with the temperature.

The observed flow and purity values are lower than the calculated ones (pure gas). In the mixture, there is competition between CH_4 and H_2 for the pores; the bigger CH_4 can block them and hinder H_2 to pass through the pores, especially at lower temperatures where CH_4 adsorption is higher (Fig. 6 b).

The flux and H_2 purity of the permeated mixtures containing 10% of H_2 (inlet and permeated pressure, 7.5 and 0.01 bar respectively) at various permeation temperatures were determined and the results are shown in Table 4 and Fig. 9a. The flow of both gases decreases with the temperature (Fig. 9a) and this decrease is more remarked for CH_4 at lower temperatures where adsorption is higher (at 30 °C, only 0.1 mL min^{-1} is observed). This is reflected in the purity obtained in the permeated (Fig. 9b), where at 30 °C almost pure H_2 is obtained (99.4%). According to the results, the H_2 purity could be increased if the permeation is carried out even at lower temperatures; these experiments were not possible to do because of the difficulty of maintaining constant the temperature during the permeation experiments in the actual setup. At 30 °C, the observed purity is higher than the calculated one according to single gas tests and this is associated to the higher contribution of the adsorbed CH_4 in the pore. Robeson's plot is constructed using selectivity from single gas permeation test; however, for comparison purposes, the calculated selectivity and permeability for the 10% H_2/CH_4 gas mixture at 30 °C (Table 4) is introduced in Fig. 8, It is observed that for the mixed gas the permeability reaches a value of 750 barrer which is lower that for single gas (1620 barrer);

Table 3 – Calculated and observed permeate flow and H_2 purity from H_2–CH_4 mixtures with different H_2 content at 40 and 80 °C[a].

Temperature [°C]	H_2 in the mix [%]	Flow calc. [mL min^{-1}]	Flow obs. [mL min^{-1}]	H_2 purity calc. [%]	H_2 purity obs. [%]
40	5	32.3	18.3	95.8	93.3
40	10	63.2	32.7	98.0	96.6
40	20	125.0	65.9	99.1	96.7
80	5	59.4	35.1	65.7	65.2
80	10	97.3	56.2	80.2	76.4
80	20	173.2	101.2	90.1	84.8

[a] Inlet pressure 7.5 bar, inlet flow 2000 mL min^{-1}, permeate pressure 0.01 atm. Calculated (calc), observed (obs).

Table 4 – Flow and Hydrogen purity of the permeate at various temperatures for a mixture containing 10% of hydrogen[a].

Temperature [°C]	Total flow [mL min^{-1}]	H_2 flow [mL min^{-1}]	CH_4 flow [mL min^{-1}]	H_2 purity calc. [%]	H_2 purity obs. [%]
30	26.7	26.6	0.1	98.0	99.4
40	32.7	31.5	1.1	97.9	96.6
60	44.3	37.8	6.5	95.1	85.4
80	56.2	42.9	13.3	80.2	76.4

[a] Inlet pressure 7.5 bar, inlet flow 2000 mL min^{-1}, permeate pressure 0.01 atm.

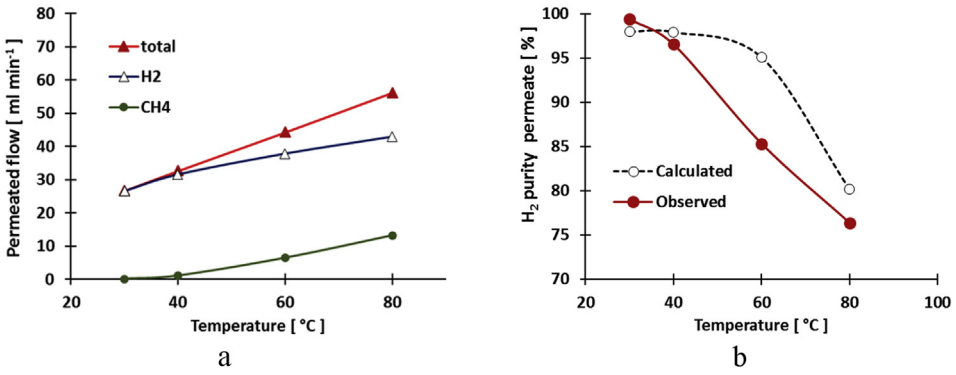

Fig. 9 – a) flow and b) hydrogen purity of the permeated at various temperatures for a mixture containing 10% of hydrogen.

Table 5 – Hydrogen and methane flow rate, and purity in the permeate at various pressures at 40 °C for a mixture containing 10% of hydrogen[a].

Total pressure Inlet [kPa]	H_2			CH_4		
	ΔP_{H2} [bar]	Flow rate [mL min^{-1}]	Purity [%]	ΔP_{CH4} [bar]	Flow rate [mL min^{-1}]	Purity [%]
7.5	0.74	31.5	96.6	6.75	1.12	3.4
7.0	0.69	30.3	98.2	6.30	0.56	1.8
6.0	0.59	25.9	98.4	5.40	0.42	1.6
5.0	0.49	22.2	99.1	4.50	0.20	0.9
4.0	0.39	19.7	99.2	3.60	0.15	0.8

[a] Pressure in the permeate 0.01 bar.

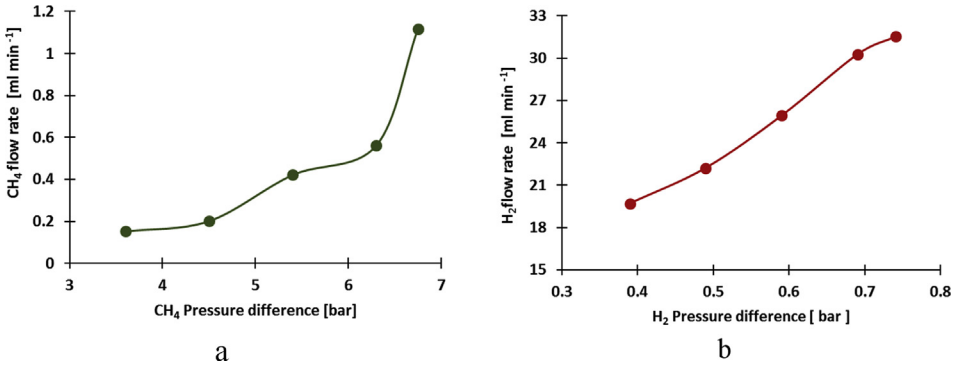

Fig. 10 – a) Methane and b) hydrogen flow rates at various trans membrane pressure differences of a mixture containing 10% of H_2 at 40 °C.

however, the selectivity reaches 1540 which is much higher that ideal selectivity for single gas (442). For mix gases, since at low temperatures CH_4 is adsorbed on the pores, the pore size is reduced. Consequently, the H_2 permeability is reduced compared to the case of single gas, but the selectivity is increased.

The effect of the feed pressure in the permeation properties of a gas mixture containing 10% of H_2 at 40 °C, while keeping the inside pressure of 0.01 bar were carried out and the results are shown in Table 5 and Fig. 10 (the difference in pressure across the membrane were calculated considering the composition in the permeate). For both gases, there is not a linear correlation between the pressure difference and the flux; in the case of methane, the flow rate increases at higher pressures, as consequence of the contribution of the adsorption diffusion mechanism of transport; at higher pressures, more methane molecules are adsorbed on the pores. The CH_4 adsorbed is reflected on the decrease of the H_2 flow. These results evidence the influence of the feed pressure on the separation properties, although it should be noted that the purity in the permeate is still high for all the cases.

Conclusions

Al-CMSM membranes carbonized at 500 °C were successfully prepared. The single gas permeation properties obtained were comparable to similar shorter membranes carbonized at 500 °C reported before, showing the reproducibility of the fabrication method. The membrane tested showed that the mechanism of gas transport is molecular sieving, in the case of non-absorbable gases. For CO_2 (at the temperatures tested),

and CH_4 at less than 60 °C, the permeation is a combination of molecular sieving and adsorption diffusion. The H_2/CH_4 permselectivity and permeability properties of the membrane are placed well above the Robeson limit of polymeric membranes.

The membrane was tested for the separation of low concentration of H_2 (5–20% by volume) in a mixture with CH_4 simulating the conditions for the separation of H_2 injected in the natural gas grid. The H_2 purity obtained changes with the temperature of permeation, composition of the mixture and *trans*-membrane pressure difference. For samples containing 10% of H_2 with inlet pressure of 7.5 and permeate pressure of 0.01 bar at 30 °C, the H_2 purity obtained was 99.4% which makes this membrane a good candidate for the separation of H_2 blended with natural gas.

Author contribution

M.A. Llosa and D.A. Pacheco performed the preparation of the membrane. J.A. Medrano, V. Cecchetto and F. Gallucci performed the gas permeation measurements. All the authors worked in drafting the work, the experimental design, and analysis of the results and the preparation of the manuscript.

Funding

This project received funding from the Fuel Cells and Hydrogen 2 Joint Undertaking under grant agreement N 700355 (Hygrid). This Joint Undertaking receives support from the European Union's Horizon 2020 Research and Innovation Programme, Hydrogen Europe and N. ERGHY.

Disclaimer

The present publication reflects only the author's views and the FCH JU is not liable for any use that may be made of the information contained therein.

Appendix A. Supplementary data

Supplementary data to this article can be found online at https://doi.org/10.1016/j.ijhydene.2020.05.088.

REFERENCES

[1] Bhandarkar M, Shelekhin AB, Dixon AG, Ma YH. Adsorption, permeation, and diffusion of gases in microporous membranes. I. Adsorption of gases on microporous glass membranes. J Membr Sci 1992;75:221–31. https://doi.org/10.1016/0376-7388(92)85065-Q.

[2] Campo MC, Magalhaes FD, Mendes A. Carbon molecular sieve membranes from cellophane paper. J Membr Sci 2010;350:180–8. https://doi.org/10.1016/j.memsci.2009.12.026.

[3] Fernandez E, Coenen K, Helmi A, Melendez J, Zuñiga J, Pacheco Tanaka DA, et al. Preparation and characterization of thin-film Pd-Ag supported membranes for high-temperature applications. Int J Hydrogen Energy 2015;40:13463–78. https://doi.org/10.1016/j.ijhydene.2015.08.050.

[4] Fernandez E, Helmi A, Medrano JA, Coenen K, Arratibel A, Melendez J, et al. Palladium based membranes and membrane reactors for hydrogen production and purification: an overview of research activities at Tecnalia and TU/e. Int J Hydrogen Energy 2017;42:13763–76. https://doi.org/10.1016/j.ijhydene.2017.03.067.

[5] Helmi A, Fernandez E, Melendez J, Tanaka DAP, Gallucci F, Van Sint Annaland M. Fluidized bed membrane reactors for ultra pure H2 production - a step forward towards commercialization. Molecules 2016;21. https://doi.org/10.3390/molecules21030376.

[6] Hosseini SS, Chung TS. Carbon membranes from blends of PBI and polyimides for N2/CH4and CO2/CH4separation and hydrogen purification. J Membr Sci 2009;328:174–85. https://doi.org/10.1016/j.memsci.2008.12.005.

[7] Kumakiri I, Tamura K, Sasaki Y, Tanaka K, Kita H. Influence of iron additive on the hydrogen separation properties of carbon molecular sieve membranes. Ind Eng Chem Res 2018;57:5370–7. https://doi.org/10.1021/acs.iecr.7b05265.

[8] Llosa Tanco MA, Pacheco Tanaka DA, Mendes A. Composite-alumina-carbon molecular sieve membranes prepared from novolac resin and boehmite. Part II: effect of the carbonization temperature on the gas permeation properties. Int J Hydrogen Energy 2 March 2015;40(8):3485–96. https://doi.org/10.1016/j.ijhydene.2014.11.025.

[9] Llosa Tanco MA, Pacheco Tanaka DA, Rodrigues SC, Texeira M, Mendes A. Composite-alumina-carbon molecular sieve membranes prepared from novolac resin and boehmite. Part I: preparation, characterization and gas permeation studies. Int J Hydrogen Energy 2015b;40:5653–63. https://doi.org/10.1016/j.ijhydene.2015.02.112.

[10] Medrano JA, Fernandez E, Melendez J, Parco M, Tanaka DAP, Van Sint Annaland M, et al. Pd-based metallic supported membranes: high-temperature stability and fluidized bed reactor testing. Int J Hydrogen Energy 2016;41:8706–18. https://doi.org/10.1016/j.ijhydene.2015.10.094.

[11] Melaina W, Antonia O, Penev M. Blending hydrogen into natural gas pipeline networks: a review of key issues. Denver, Colorado technical report NRL/TP 5600-51995. 2013.

[12] Melendez J, de Nooijer N, Coenen K, Fernandez E, Viviente JL, van Sint Annaland M, et al. Effect of Au addition on hydrogen permeation and the resistance to H2S on Pd-Ag alloy membranes. J Membr Sci 2017a;542:329–41. https://doi.org/10.1016/j.memsci.2017.08.029.

[13] Melendez J, Fernandez E, Gallucci F, van Sint Annaland M, Arias PL, Pacheco Tanaka DA. Preparation and characterization of ceramic supported ultra-thin (~1 μm) Pd-Ag membranes. J Membr Sci 2017b;528:12–23. https://doi.org/10.1016/j.memsci.2017.01.011.

[14] Ngamou PHT, Ivanova ME, Guillon O, Meulenberg WA. High-performance carbon molecular sieve membranes for hydrogen purification and pervaporation dehydration of organic solvents. J Mater Chem A 2019;7:7082–91. https://doi.org/10.1039/c8ta09504c.

[15] Okazaki J, Tanaka DAP, Tanco MAL, Wakui Y, Mizukami F, Suzuki TM. Hydrogen permeability study of the thin Pd-Ag alloy membranes in the temperature range across the α-β phase transition. J Membr Sci 2006;282:370–4. https://doi.org/10.1016/j.memsci.2006.05.042.

[16] Pacheco Tanaka DA, Llosa Tanco MA, Niwa SI, Wakui Y, Mizukami F, Namba T, et al. Preparation of palladium and silver alloy membrane on a porous ??-alumina tube via

simultaneous electroless plating. J Membr Sci 2005;247:21–7. https://doi.org/10.1016/j.memsci.2004.06.002.

[17] Shelekhin AB, Dixon AG, Ma YH. Theory of gas diffusion and permeation in inorganic molecular???sieve membranes. AIChE J 1995;41:58–67. https://doi.org/10.1002/aic.690410107.

[18] Teixeira M, Campo MC, Pacheco Tanaka DA, Llosa Tanco MA, Magen C, Mendes A. Composite phenolic resin-based carbon molecular sieve membranes for gas separation. Carbon N. Y. 2011;49:4348–58. https://doi.org/10.1016/j.carbon.2011.06.012.

[19] Teixeira M, Campo M, Pacheco Tanaka DA, Llosa Tanco MA, Magen C, Mendes A. Carbon–Al2O3–Ag composite molecular sieve membranes for gas separation. Chem Eng Res Des 2012;90:2338–45. https://doi.org/10.1016/j.cherd.2012.05.016.

[20] Teixeira M, Rodrigues SC, Campo M, Pacheco Tanaka DA, Llosa Tanco MA, Madeira LM, et al. Boehmite-phenolic resin carbon molecular sieve membranes-Permeation and adsorption studies. Chem Eng Res Des 2014;92. https://doi.org/10.1016/j.cherd.2013.12.028.

[21] Tseng HH, Wang CT, Zhuang GL, Uchytil P, Reznickova J, Setnickova K. Enhanced H2/CH4and H2/CO2separation by carbon molecular sieve membrane coated on titania modified alumina support: effects of TiO2intermediate layer preparation variables on interfacial adhesion. J Membr Sci 2016;510:391–404. https://doi.org/10.1016/j.memsci.2016.02.036.